ELSEVIER

Applied Catalysis A: General 215 (2001) 21–30

APPLIED CATALYSIS A: GENERAL

www.elsevier.com/locate/apcata

Sulfated zirconia catalyst supported on MCM-41 mesoporous molecular sieve

Chang-Lin Chen [a,b], Soofin Cheng [a], Hong-Ping Lin [c], She-Tin Wong [a], Chung-Yuan Mou [a,*]

[a] *Department of Chemistry, National Taiwan University, Taipei 106, Taiwan*
[b] *Department of Chemical Engineering, Nanjing University of Chemical Technology, Nanjing 210009, China*
[c] *Institute of Atomic and Molecular Sciences, Academia Scinica, Taipei, Taiwan*

Received 8 November 2000; received in revised form 22 January 2001; accepted 24 January 2001

Abstract

Sulfated zirconia (SZ) was supported on siliceous hollow tubular MCM-41 mesoporous molecular sieve by using a one-step incipient wetness impregnation method with zirconium sulfate as the precursor. The SZ/MCM-41 catalyst was obtained by thermal decomposition of the precursor in air. The resultant catalyst was characterized with various techniques, such as nitrogen physisorption, X-ray diffraction, SEM, and TEM. It was shown that the well-ordered channels of MCM-41 support arranged in hexagonal arrays while the hollow tubular morphology was retained. Both tetragonal and monoclinic phases of zirconia were developed in the catalysts. With the addition of a proper amount of aluminum as a promoter, resulting in catalyst SZA/MCM-41, the transformation of zirconia from metastable tetragonal phase to monoclinic phase was retarded. The catalytic activity of SZA/MCM-41 catalyst in the isomerization of *n*-butane was dramatically improved in comparison to the activities of SZ/MCM-41 or SZA/silica.

Keywords: Sulfated zirconia; Molecular sieve; MCM-41; Isomerization of *n*-butane

1. Introduction

Due to the hazardous properties of liquid acids such as HF and H_2SO_4 commonly employed in the current petrochemical industry, a great effort has been focused on the development of more environmentally friendly strong solid acids [1]. Sulfated metal oxides, especially sulfated zirconia (abbreviated as SZ), have attracted great attention in the past few years because they demonstrate high catalytic activities in skeletal isomerization of alkanes at relatively low temperatures [2–4]. The catalytical activity of sulfated zirconia significantly depends upon the preparation method and the activating treatment. Many recent works have been devoted to finding various methods of the catalyst preparation. Recently, Yadav and Nair have published a detailed review on the effects of various preparation parameters of S-ZrO_2 [5].

One of the main factors which controlled the catalytic activity of SZ was the surface area and thus the sulfur content on the surface [6]. The SZ catalysts prepared properly could achieve surface areas around 100–120 m^2/g. For pure zirconia, the surface area is usually controlled by the temperature of calcination [7]. However, the material generally suffered from texture inhomogeneity and low thermal stability, so that upon sulfation only a portion of sulfur is present on the

* Corresponding author. Fax: +886-2-23660954.
E-mail address: cymou@ms.cc.ntu.edu.tw (C.-Y. Mou).

0926-860X/01/$ – see front matter
PII: S0926-860X(01)00504-X

external surface as active sites [6]. The preparation of porous zirconia of high surface areas has been reported [8–11]. However, upon calcination around 600°C prior to catalytic testing, the surface areas of these samples shrank to values similar to or lower than the conventional zirconia samples. Improvement of structural stability of zirconia has been carried out by impregnation of zirconia on thermally resistant supports such as silica [12–15]. However, depending on the preparation method, diffusion of zirconia in the silica support or vice versa was observed and the resultant materials were often surface-heterogeneous composites.

As for the catalytic activity of S-ZrO_2, another important factor may be the mesopore volume. Recently, Wolf and Risch [16] prepared catalyst by refluxing the materials and obtained SZ catalysts with high mesopore volume (0.4 cm^3/g). They found much higher conversion in butane isomerization with this reflux catalyst compared to results with a conventional catalyst with low mesopore volume.

Thus, it is desirable to prepare stable and homogeneous SZ catalysts with high mesopore volume. For this purpose, SZ supported on a mesoporous material seems to be desirable. The development of supported SZ with improved characteristics such as high surface area, high mesopore volume, and homogeneous dispersion is carried out in the present study by using mesoporous molecular sieve MCM-41 as the support.

MCM-41 is the most well-studied members of the M41S meso-structured family discovered by the researchers at Mobil [17]. It has a uniform hexagonal array of mesopores and very high surface area (typically around 1000 m^2/g or higher). This material has been shown to be an excellent support for preparing supported catalysts with activities and selectivities superior to those over amorphous silica, alumina, and even zeolites [18–20].

In the last few years, MCM-41 materials with hollow tubular morphology have been synthesized in our laboratory by careful control of the surfactant-water content and the silica condensation rate [21–23], and by addition of some organic molecules during the synthesis [24]. One of the advantages of the hollow tubular siliceous MCM-41 is that its porous structure and morphology are thermally stable at least to 800°C. In addition, there are always defect holes, with pore diameter ca. 5–30 nm, amid the nanochannels in the tubular MCM-41, which make the hexagonal array of mesopores become effectively interconnected [25]. These defects facilitate the material transport and enhance catalytic conversions. The effect of the morphology of MCM-41 as support was examined in dehydrogenation of ethylbenzene to styrene over supported molybdenum oxide catalysts [26]. The tubular MCM-41 catalyst physically mixed with molybdenum oxide gave higher conversion in styrene formation than the particulate catalysts [26]. The catalytic performance was interpreted in terms of the effective surface area, and in particular the facility of diffusion of the reactant and product molecules through the interconnected channels of the tubular MCM-41 support. These interconnected channels also contribute to the activities of the tubular MCM-41 catalysts being higher than those of particulate catalysts in hydrodesulfurization of VGO carried out in a trickle bed reactor using MCM-41 catalysts loaded with 12 wt.% MoO_3 and 3 wt.% NiO [27].

In this research, sulfated zirconia supported on hollow tubular pure siliceous MCM-41 was prepared, using zirconium sulfate as the precursor. The acid properties of the resultant catalysts were characterized with TPD of benzene and by studying their catalytic activities in *n*-butane isomerization reaction.

2. Experimental

2.1. Preparation of hollow tubular pure siliceous MCM-41

Hollow tubular pure siliceous MCM-41 was synthesized with the delayed neutralization process reported by Lin et al. [22]. A given amount of acetone was dissolved into a cetyltrimethylammonium bromide (C_{16}TABr) aqueous solution to form a clear solution and then sodium silicate was added. After stirring for about 10 min at 30°C, a 1.2 M H_2SO_4 aqueous solution was added dropwise to the gel mixture to acidify the reaction system. Typically, the time required for complete acidification is about 30–45 min. The molar composition of the resultant gel is 1.0 M C_{16}TABr:2.0 M SiO_2:0.8 M Na_2O:0.67 M H_2SO_4:1.0 M acetone:133 M H_2O. The gel was crystallized in static condition at 100°C for 5 days. Then the solid product was filtered, washed with deionized water, dried, and finally calcined at 560°C for 6 h in

static air to remove the organic template. XRD analysis of the calcined product showed a typical pattern for well-ordered MCM-41. SEM technique confirmed its hollow tubular morphology. From N_2 adsorption–desorption isotherms, this material was found to have a BET surface area of 1019 m^2/g, uniform pores of 2.46 nm in diameter, and a pore volume of 0.92 ml/g.

2.2. Preparation of SZ/MCM-41, SZA/MCM-41, and SZA/SiO_2 catalysts

Hollow tubular pure siliceous MCM-41 was impregnated with a desired amount of $Zr(SO_4)_2$ in methanol solution by the incipient wetness method. The resulting sample was dried at 120°C for 12 h. Finally, it was calcined at 700°C for 3 h in air. The calcined form is designated as SZ/MCM-41. Al-promoted samples were prepared in the same way with the desired amount of zirconium sulfate and aluminum sulfate mixture. The calcined form is designated as SZA/MCM-41.

In order to compare the nature of the support, a sulfated zirconia with aluminum promoter supported on amorphous silica was also prepared and designated as SZA/SiO_2 catalyst.

2.3. Catalyst characterization

2.3.1. X-ray diffraction

XRD measurements were carried out on a Scintag X1 diffractometer using Cu Kα radiation ($\lambda = 0.154$ nm). The XRD patterns were recorded from 1.5 to 70° (2θ) in steps of 0.02° with a count time of 0.5 s at each step.

2.3.2. N_2 adsorption–desorption

The BET surface area and pore volume of all the samples were determined with a Micromeritics ASAP 2000 apparatus using nitrogen as the analysis gas. Prior to analysis, each sample was outgassed overnight at 300°C under 10^{-3} Torr. The pore-size distribution curves were obtained from the analysis of the desorption portion of the isotherms using the BJH (Barrett–Joyner–Halenda) method.

2.3.3. Scanning electron microscopy (SEM) and transmission electron microscopy (TEM)

SEM and TEM were used to study the morphology and pore structures of the catalysts. SEM was performed on a Hitachi S-2400 instrument using an accelerating voltage of 20 keV. TEM was performed on a Hitachi H-7100 instrument operated at 100 keV.

2.3.4. Temperature-programmed desorption of benzene

The temperature-programmed desorption (TPD) of benzene was performed in order to determine the distribution of strong acid sites on the catalysts. The analysis was conducted in a conventional flow system. The carrier gas used was He, flowing at a rate of 60 ml/min. The desorption process was monitored by a TCD detector. About 0.2 g of the calcined catalyst was used for each experiment. Prior to the analysis, the catalyst sample was pretreated in situ for 2 h in a He flow (30 ml/min) at 450°C. Adsorption of benzene was performed by passing a He stream with benzene vapor over the catalyst for 30 min. The adsorption process was carried out at 110°C in order to eliminate physically adsorbed benzene. After the adsorption of benzene, the sample was flushed with the carrier gas at 110°C for another 1 h. The TPD profile of benzene was obtained from 110 to 650°C at a heating rate of 10°C/min.

2.3.5. Solid-state NMR

Solid-state ^{27}Al MAS NMR spectra were taken to determine the coordination states of aluminum. The experiments were performed at room temperature on a Bruker DSX400 WB NMR spectrometer. A 1 mol/dm^3 $Al(NO_3)_3$ solution was used as the external reference.

2.3.6. Sulfur content

The bulk sulfur content in the calcined catalysts was determined by inductively coupled plasma atomic emission spectrometry (ICP-AES) using a Jarrel-Ash ICAP 9000 instrument. The surface sulfur content was determined by X-ray photoelectron spectroscopy (XPS) using a VG Microteck MT 500 instrument.

2.3.7. Catalytic studies

The isomerization of *n*-butane to isobutane was performed in a fixed-bed continuous flow reactor. The reactor was operated at atmospheric pressure. The catalyst samples were pelletized and sized to 20/60 mesh. Approximately 0.5 g of the catalyst was loaded into the reactor and then pretreated for 3 h in flowing

dry air (60 ml/min) at 450°C. The reactor temperature was then lowered to the reaction temperature of 250°C. After thermal equilibrium was established, the reaction was started by feeding *n*-butane/H_2 mixture (1:10 v/v) at *n*-butane weight hourly space velocity (WHSV) of 1.05 h^{-1} through the catalyst. The flow of the feed gas was monitored using a Brooks mass flow controller. The reaction products were analyzed by a Shimadzu 14B gas chromatograph with a 60 m DB-1 column and FID detector.

3. Results and discussion

3.1. Characterization of SZ/MCM-41 and SZA/MCM-41 catalysts

3.1.1. XRD analysis

Fig. 1 shows the XRD patterns of pristine hollow tubular pure siliceous MCM-41 and the SZ/MCM-41 catalysts with various SZ loadings. The starting MCM-41 has a typical XRD pattern for 2D hexagonal mesophase. It exhibits a very strong (1 0 0) diffraction peak at a *d*-spacing of 3.99 nm and three other weaker peaks corresponding to (1 1 0), (2 0 0), and (2 1 0) reflections.

The XRD patterns of SZ/MCM-41 catalyst also showed the four typical diffraction peaks in the low 2θ region. This indicates that the regular arrangement of mesoporous structure of MCM-41 is preserved in SZ/MCM-41. However, the intensity of the four peaks indexed with a hexagonal lattice decreases as the SZ content increases. In order to maintain the porous structure in SZ/MCM-41, a moderate SZ content (about 18 wt.% of Zr) was used for the catalytic studies hereafter. Moreover, since very weak and broad diffraction due to ZrO_2 crystallites was observed on the XRD patterns, SZ should be well dispersed on the MCM-41 surface. After calcination at 700°C, the zirconium sulfate impregnated on hollow tubular pure siliceous MCM-41 decomposed and formed zirconia in both tetragonal and monoclinic phases. It has been reported by many researchers that the sulfated monoclinic zirconia is less catalytically active than the tetragonal phase [28–31]. Recently, Gao et al. discovered that the catalytic activity of sulfated zirconia could be enhanced by the addition of Al_2O_3 [32,33]. They concluded that the presence of Al_2O_3 could retard the transformation of the metastable tetragonal phase to the thermodynamically favored monoclinic phase. The intensity of the tetragonal zirconia and the sulfur content was found to increase with Al_2O_3 content. In the present work, aluminum was also incorporated into the SZ/MCM-41 catalysts in order to study the promotion effect. Fig. 2 shows the XRD patterns of SZA/MCM-41 with various Al contents. Different from that observed by Gao et al., a pure tetragonal zirconia phase was obtained at 700°C only

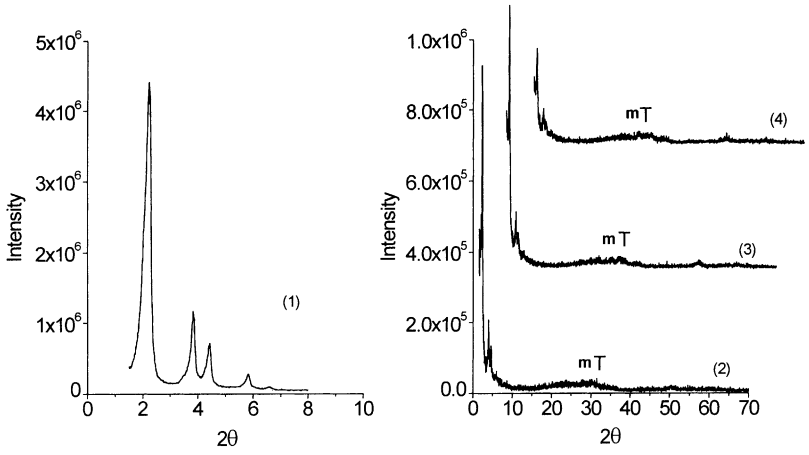

Fig. 1. XRD patterns of SZA/MCM-41 with various $Zr(SO_4)_2$/MCM-41 ratio calcined at 700°C for 3 h (m: monoclinic phase; T: tetragonal phase): (1) MCM-41; (2) $Zr(SO_4)_2$/MCM-41 = 1.0 (g/g); (3) $Zr(SO_4)_2$/MCM-41 = 1.2 (g/g); (4) $Zr(SO_4)_2$/MCM-41 = 1.4 (g/g).

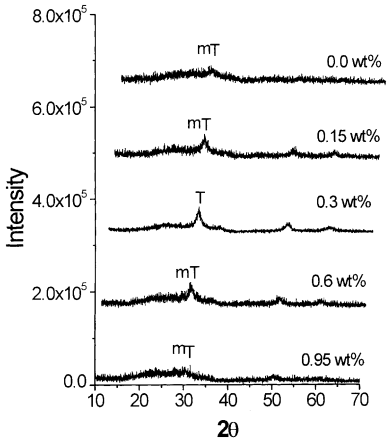

Fig. 2. XRD patterns of SZA/MCM-41 with different Al contents calcined at 700°C for 3 h. All the samples have the same starting $Zr(SO_4)_2$/MCM-41 ratio of 1.0 (g/g) (m: monoclinic phase; T: tetragonal phase).

when a proper amount (0.3 wt.%) of aluminum was also incorporated with zirconium sulfate on MCM-41.

3.1.2. Physico-chemical properties of the catalysts

Table 1 compares the sulfur content, surface area, and total pore volume of SZ/MCM-41, SZA/MCM-41, and SZA/SiO_2 calcined at 700°C. Hollow tubular pure siliceous MCM-41 has a BET surface area greater than 1000 m^2/g. It can be seen that the BET surface area and pore volume of SZA/MCM-41 are smaller than those of MCM-41. Even so, a typical SZA/MCM-41 sample can reach a surface area of more than 500 m^2/g (shown in Table 1). The BET surface area and pore volume of SZA/MCM-41 are slightly greater than those of SZ/MCM-41. Moreover, the sulfur content, either in the bulk or on the surface, of SZA/MCM-41 is significantly higher than that of SZ/MCM-41. This implies that the Al in SZA/MCM-41 helps to stabilize the sulfur in the structure and surface remarkably. In comparison with that of SZA/SiO_2, the sulfur content in SZA/MCM-41 is also higher.

Fig. 3 shows the representative N_2 adsorption–desorption isotherms of hollow tubular pure siliceous MCM-41 and SZA/MCM-41. The isotherms are similar in shape and both are type IV curves. This indicates that the ordering of the hexagonal arrays of mesopores in MCM-41 was not much affected. However, the position of the capillary condensation step shifted slightly towards lower partial pressure. The corresponding pore-size distributions determined by BJH method are also shown in Fig. 3. SZA/MCM-41 exhibits less pore volume, slightly broader pore-size distribution, and smaller pore diameters than those of pristine MCM-41. These results imply that most of the SZA species were located inside the pore channels.

SEM and TEM of SZA/MCM-41 catalysts are shown in Figs. 4 and 5, respectively. The SEM photograph shows that SZA/MCM-41 is still in the tubular morphology. The diameter of the tubules is rather uniform. From the TEM micrograph of SZA/MCM-41, well-ordered channels with continuous walls are clearly observed.

3.1.3. ^{27}Al MAS NMR analysis

^{27}Al MAS NMR is the most revealing method for examining the coordination state of aluminum. Fig. 6 shows the ^{27}Al MAS NMR spectra of SZA/MCM-41 and SZA/SiO_2. No peak at about 50 ppm can be observed in either sample, indicating that the Al atoms are in octahedral coordination. This implies that Al is unlikely to be incorporated in the framework of MCM-41.

Table 1
Physico-chemical properties of the supported catalysts and the supports

Sample	Surface area (m^2/g)	Pore diameter (nm)	Pore volume (ml/g)	Content (wt.%)		S/Zr atomic ratio	
				Zr	Al	Bulk	Surface
MCM-41	1019	2.46	0.92	–	–	–	–
SiO_2 gel	525	Irregular	–	–	–	–	–
SZ/MCM-41	488	2.18	0.39	18.2	0	0.279	0.394
SZA/MCM-41	517	2.14	0.41	17.2	0.315	0.565	0.672
SZA/SiO_2	247	Irregular	–	18.2	0.315	0.315	0.479

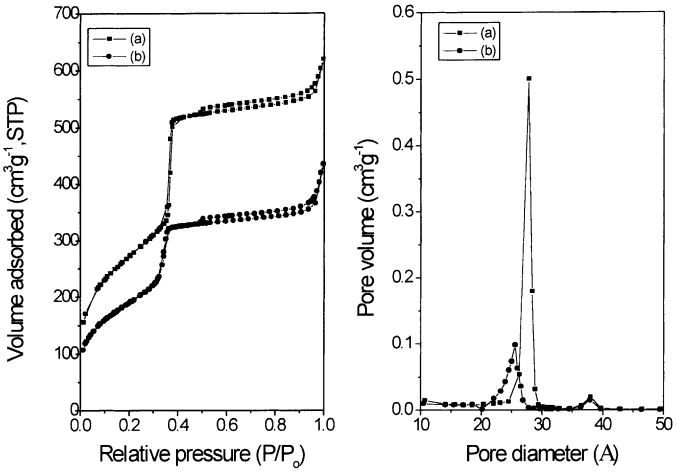

Fig. 3. Nitrogen adsorption–desorption isotherms and pore-size distribution profiles of hollow tubular pure siliceous MCM-41 and a typical calcined sample of SZA/MCM-41. $Zr(SO_4)_2$/MCM-41 ratio = 1.0 (g/g); Al content = 0.3 wt.%.

3.1.4. Temperature-programmed desorption of benzene

The benzene TPD profiles of MCM-41, SZA/MCM-41, and SZA/SiO_2 are compared in Fig. 7. Benzene is a weak base and adsorbs mostly on strong acid sites. TPD of benzene has been used to show the distribution of strong acid sites on catalysts [34,35]. Benzene desorption temperature corresponds to the strength of the acid sites present on the catalysts. Higher benzene desorption temperature implies stronger acid sites. On MCM-41, there is no detectable desorption peak. This indicates that no strong acid sites are present on MCM-41. SZA/MCM-41 and SZA/SiO_2 show a profile characterized by two resolved maxima centered at 250 and 310°C, respectively. These results suggest that both SZA/MCM-41

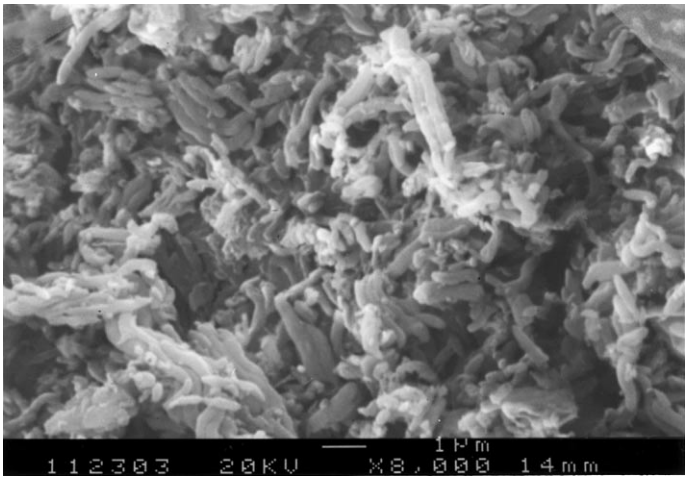

Fig. 4. Scanning electron micrograph showing the morphology of SZA/MCM-41 calcined at 700°C for 3 h. $Zr(SO_4)_2$/MCM-41 ratio = 1.0 (g/g); Al content = 0.3 wt.%.

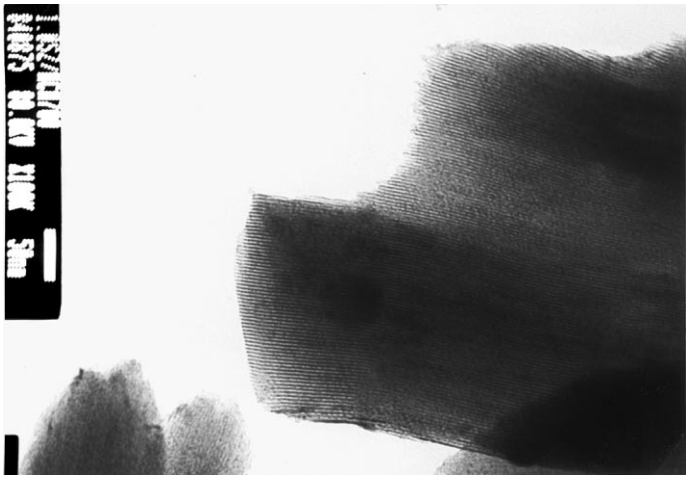

Fig. 5. Transmission electron micrograph of SZA/MCM-41 calcined at 700°C for 3 h. $Zr(SO_4)_2$/MCM-41 ratio = 1.0 (g/g); Al content = 0.3 wt.%.

and SZA/SiO_2 contain acid sites of two different strengths. Moreover, SZA/MCM-41 has a larger amount of stronger acid sites than SZA/SiO_2.

3.2. Catalytic reactions

Isomerization of *n*-butane to isobutane (see Eq. (1)) was chosen as a model reaction to test the activity of SZ/MCM-41 and SZA/MCM-41 catalysts. This reaction is catalyzed by the acid sites on the catalyst. The nature and strength of the acid sites present are expected to influence the conversion and product distribution of this isomerization reaction.

The major product of *n*-butane isomerization reaction is isobutane. The main by-products are propane and isopentane. The selectivities of isobutane obtained on SZ catalysts with and without supports are over 90%. Catalytic performance was evaluated in terms of *n*-butane conversion (Eq. (2)) and isobutane selectivity (Eq. (3)); here, *X* is *n*-butane conversion

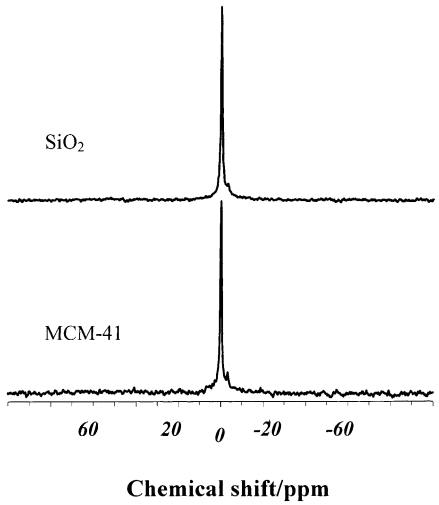

Fig. 6. The ^{27}Al NMR spectra of: (a) SZA/MCM-41; (b) SZA/SiO_2. All the samples were calcined at 700°C for 3 h. $Zr(SO_4)_2$/MCM-41 ratio = 1.0 (g/g); $Zr(SO_4)_2$/SiO_2 ratio = 1.0 (g/g); Al content = 0.3 wt.%.

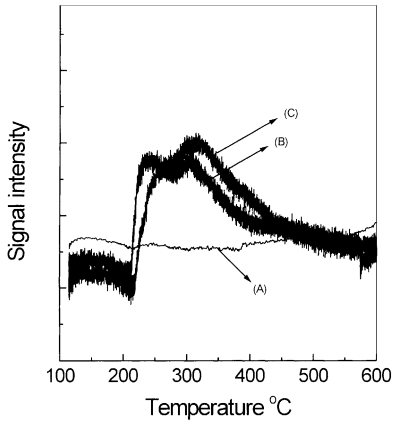

Fig. 7. Benzene TPD spectra of: (A) MCM-41; (B) SZA/SiO_2; (C) SZA/MCM-41.

in percentage, S isobutane selectivity in percentage, $m_{n,\mathrm{f}}$ the mass flow rate of n-butane in the feed, $m_{n,\mathrm{p}}$ the mass flow rate of n-butane in the product, and $m_{i,\mathrm{p}}$ the mass flow rate of isobutane in the product.

$$n\text{-}C_4H_{10} \leftrightarrow i\text{-}C_4H_{10} \quad (1)$$

$$X = 100 \times \frac{(m_{n,\mathrm{f}} - m_{n,\mathrm{p}})}{m_{n,\mathrm{f}}} \quad (2)$$

$$S = 100 \times \frac{m_{i,\mathrm{p}}}{(m_{n,\mathrm{f}} - m_{n,\mathrm{p}})} \quad (3)$$

3.2.1. Effect of Al in SZA/MCM-41 on catalytic performance

Fig. 8 shows the effect of Al incorporated in SZ/MCM-41 catalyst on n-butane isomerization at 250°C. The n-butane conversion increases with the Al content up to 0.3 wt.%, and then decreases as the Al content is further increased. This trend is consistent with the variation of zirconia phase observed in XRD results. A pure tetragonal zirconia phase was obtained at 700°C when 0.3 wt.% of aluminum was incorporated with zirconium sulfate on MCM-41. The intensity of the tetragonal zirconia phase decreases when either less or more Al is introduced. Accordingly, the promotion effect of Al is probably due to the fact that Al may stabilize the metastable tetragonal zirconia phase, and the latter then may contribute to the surface acid sites.

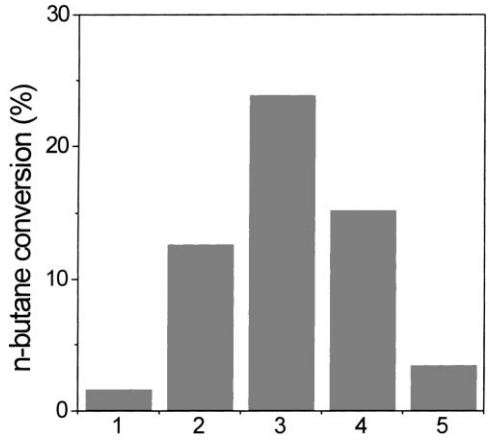

Fig. 8. The n-butane isomerization activity as a function of Al content in SZA/MCM-41: (1) 0.0 wt.%; (2) 0.15 wt.%; (3) 0.3 wt.%; (4) 0.6 wt.%; (5) 0.9 wt.%.

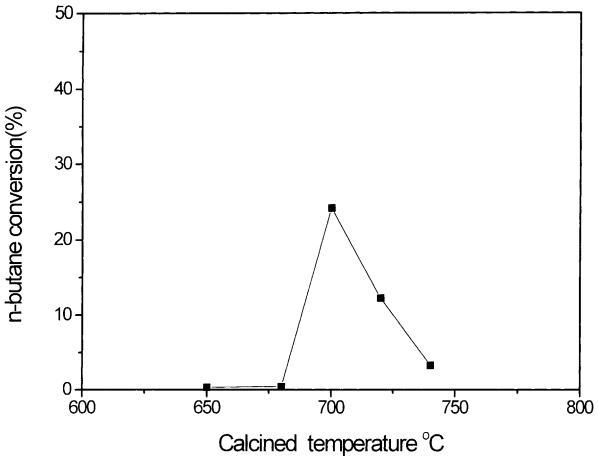

Fig. 9. Catalytic activity of SZA/MCM-41 calcined at various temperatures.

3.2.2. Effect of calcination temperature of SZA/MCM-41 on catalytic performance

The calcination temperature used for preparation of SZA/MCM-41 catalyst has a significant effect on the catalytic activity of n-butane isomerization. Fig. 9 shows the dependence of butane conversion on calcination temperature. The optimal activity was observed on the catalyst calcined at 700°C; n-butane conversion of about 25% is reached in this case. The catalysts calcined at or below 680°C have very low activities in n-butane isomerization. Similar low activity was also observed for the catalyst calcined at 740°C. Therefore, the formation of active sites on SZA/MCM-41 is strongly dependent on the decomposition temperature of $Zr(SO_4)_2$.

Decomposition of zirconium sulfate forms zirconia and releases SO_3. At the same time, some sulfate ions are retained on the surface. The interaction between the retained sulfate ions and the tetragonal zirconium oxide is proposed to form the active acid sites. When the calcination temperature is at or below 680°C, zirconium sulfate and aluminum sulfate are probably not completely decomposed. When the calcination temperature is at or above 740°C, the amount of surface-retained sulfate ions is probably low. As a result, the optimal temperature

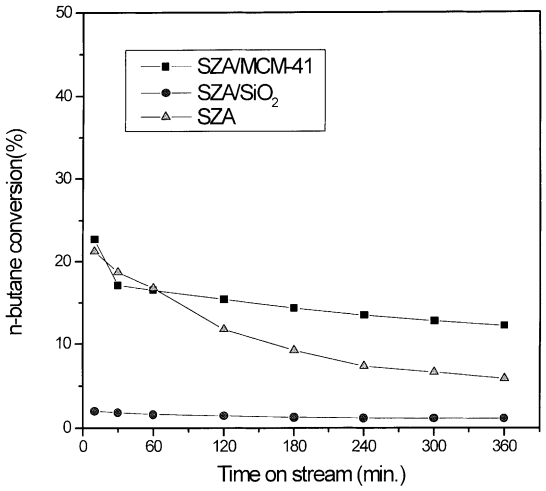

Fig. 10. Variation of the catalytic activity for *n*-butane isomerization with time-on-stream.

for the formation of sulfated tetragonal zirconia is 700°C.

3.2.3. Comparison of the performance of SZA/MCM-41, SZA/SiO_2, and SZA catalysts

SZA/MCM-41 is a new and strong solid acid with greater than 500 m^2/g surface area and regular pore-size distribution. SZA/SiO_2 is a SiO_2-supported SZA, which has irregular pore-size distribution. SZA is a typical bulk catalyst prepared by a method similar to that of Gao et al. [32]. These three catalysts have the same Al/Zr ratio. The purpose of this comparison is to check the effect of mesopores and high surface area on the catalytic activity in *n*-butane isomerization.

The *n*-butane conversion versus time-on-stream is shown in Fig. 10 for SZA/MCM-41, SZA/SiO_2, and SZA. Similar trends were observed for SZA/MCM-41 and SZA, while SZA/SiO_2 gave only trace activity. The bulk SZA catalyst shows the characteristic decay in activity. Although, SZA/MCM-41 shows the same conversion as bulk SZA during the initial stage of reaction, it achieves substantially higher conversion after 2 h on stream.

Even though, SZA/MCM-41 has twice as wide surface area as SZA/SiO_2 has, these catalytic results cannot be interpreted simply by surface area. From Table 1, one can see that SZA/MCM-41 contains more sulfur on the surface; suggesting that surface sulfur content may be an important factor other than total surface area in generating higher isomerization activity. TPD profiles of benzene also showed that the amount of acid sites in SZA/MCM-41 is slightly greater than that in SZA/SiO_2 and the acid strength of the former is stronger than that of the latter. However, the *n*-butane conversion is apparently not proportional to the amount of acid sites on the catalysts. Because the surface area of the support decreases markedly when SZA is loaded, the very low catalytic activity of SZA/SiO_2 is probably due to the fact that many small SZ crystallites fill the small pores of silica gel and so they cannot effectively catalyze the isomerization reaction. A similar phenomenon is less likely to occur on SZA/MCM-41, because MCM-41 has regular mesopores. Besides, the XRD results show that the characteristic zirconia tetragonal (1 1 1) peak at $2\theta = 30.2^\circ$ in SZA/MCM-41 is less intense than that in SZA/SiO_2. In other words, the particle size of crystalline zirconia dispersed on MCM-41 is smaller than that on silica gel. This clearly indicates that the high surface area and mesoporous pore volume of MCM-41 can help better dispersion of zirconia and can prevent the sintering of small tetragonal sulfated zirconia into large crystallites. Therefore, the good dispersion of small crystallites of sulfated tetragonal zirconia should be another important factor in generating large amount of acid sites and high isomerization activity.

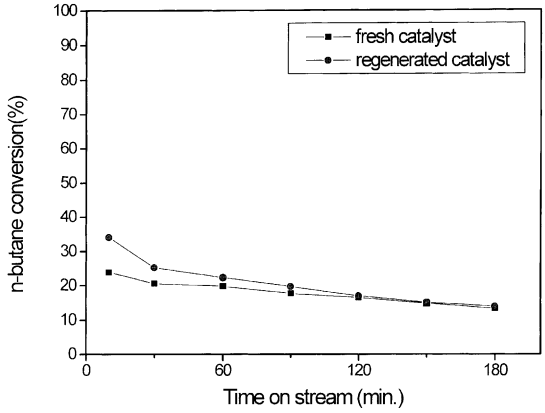

Fig. 11. The catalytic activities of fresh and regenerated catalyst SZA/MCM-41. Regeneration conditions: heating in dry air at 450°C for 3 h.

In order to evaluate the cause of SZA/MCM-41 catalyst deactivation, the deactivation and regeneration cycle of the catalyst was studied and results are illustrated in Fig. 11. SZA/MCM-41 catalyst can recover its activity completely after being treated in flowing air at 450°C for 3 h. This result demonstrates that the deactivation process is mainly caused by coke deposited on the catalyst surface.

4. Conclusions

For the first time, strong solid acid catalysts comprising of pure siliceous MCM-41 with hollow tubular morphology and sulfated zirconia have been prepared and characterized. These materials have strong acid sites generated by the well-dispersed sulfated tetragonal zirconia. Introduction of small amounts of aluminum enhances the catalytic activity of SZ/MCM-41 in *n*-butane isomerization, mainly because Al stabilizes the metastable tetragonal zirconia phase. TPD profiles of benzene showed that the amount of acid sites in SZA/MCM-41 is slightly greater than that in SZA/SiO_2, and the acid strength of the former is also stronger than that of the latter. However, SZA/SiO_2 gave very low catalytic activity in *n*-butane isomerization. This may be because many of the SZ crystallites are trapped inside the small pores of silica gel and cannot effectively catalyze the isomerization reaction. The advantages of SZA/MCM-41 as a catalyst are its rather large surface area and most importantly its mesopores of narrowly distributed size, which help the formation of small SZ crystallites homogeneously dispersed on the support. These mesoporous catalysts are particularly useful for catalytic reactions involving organic compounds of large molecular sizes.

Acknowledgements

We thank Dr. Shang-Bin Liu, Institute of Atomic and Molecular Sciences, Academia Scinica, and Prof. Ben-Zu Wan, Department of Chemical Engineering, National Taiwan University, for helpful discussions. The financial support from China Petroleum Corporation, Taiwan, is gratefully acknowledged.

References

[1] A. Corma, A. Martinez, Catal. Rev.-Sci. Eng. 35 (1993) 483.
[2] A. Corma, Chem. Rev. 95 (1995) 559.
[3] B.H. Davis, R.A. Keogh, R. Srinivasan, Catal. Today 20 (1994) 219.
[4] X. Song, A. Sayari, Catal. Rev.-Sci. Eng. 38 (1996) 329.
[5] G.D. Yadav, J.J. Nair, Microporous Mesoporous Mater. 33 (1999) 1.
[6] V. Parvulescu, S. Cman, V.I. Parvulescu, P. Grange, G. Poncelet, J. Catal. 180 (1998) 66.
[7] K. Tanabe, Y. Nakano, T. Eizuka, H. Hattori, J. Catal. 57 (1979) 1.
[8] T. Lopez, R. Gomez, G. Ferrat, J.M. Dominguez, I. Schifter, Chem. Lett. (1992) 1941.
[9] D.R. Acosta, O. Novaro, T. Lopez, R. Gomez, J. Mater. Res. 10 (1995) 1397.
[10] T. Lopez, M. Asomoza, R. Gomez, Thermochim. Acta 223 (1993) 233.
[11] R. Gomez, T. Lopez, F. Tzompantzi, E. Garciafigueroa, D.W. Acosta, O. Novara, Langmuir 13 (1997) 970.
[12] D.A. Ward, E.I. Ko, Chem. Mater. 5 (1993) 956.
[13] U. Ciesla, S. Schacht, G.D. Stucky, K.K. Unger, F. Schuth, Angew. Chem. Int. Ed. Engl. 35 (1996) 541.
[14] E.C. Subbarao, Science and Technology of Zirconia, American Ceramic Society, Columbus, OH, 1981, p. 1.
[15] M.S. Wong, J.Y. Ying, Chem. Mater. 10 (1998) 2067.
[16] E.E. Wolf, M.A. Risch, Appl. Catal. A 172 (1998) L1.
[17] C.T. Kresge, M.E. Leonowicz, W.J. Roth, J.C. Vartuli, J.S. Beck, Nature 359 (1992) 710.
[18] A. Corma, A. Martinez, V. Martinez-Soria, J.B. Monton, J. Catal. 153 (1995) 25.
[19] A. Corma, A. Martinez, V. Martinez-Soria, J. Catal. 169 (1997) 480.
[20] T. Ookoshi, M. Onaka, Chem. Commun. (1998) 2399.
[21] H.P. Lin, C.Y. Mou, Science 273 (1996) 765.
[22] H.P. Lin, S. Cheng, C.Y. Mou, Microporous Mater. 10 (1997) 111.
[23] H.P. Lin, S. Cheng, C.Y. Mou, Chem. Mater. 10 (1998) 581.
[24] H.P. Lin, Y.R. Cheng, S.B. Liu, C.Y. Mou, J. Mater. Chem. 9 (1999) 1197.
[25] H.P. Lin, S.T. Wong, C.Y. Mou, C.Y. Tang, J. Phys. Chem. B 104 (2000) 8967.
[26] S.T. Wong, H.P. Lin, C.Y. Mou, Appl. Catal. A: Gen. 198 (2000) 103.
[27] T.R. Lin, B. Wan, H.P. Lin, C.Y. Mou, Technical Report to China Petroleum Co., 1998.
[28] M. Hino, S. Kobayashi, K. Arata, J. Am. Chem. Soc. 101 (1979) 6439.
[29] K. Arata, Adv. Catal. 37 (1990) 165.
[30] T. Yamaguchi, Appl. Catal. 61 (1990) 1.
[31] C. Morterra, G. Cerrato, F. Pinna, M. Signoretto, J. Catal. 157 (1995) 109.
[32] Z. Gao, Y. Xia, W. Hua, C. Miao, Topics in Catal. 6 (1998) 101.
[33] Y. Xia, W. Hua, Z. Gao, Appl. Catal. A: Gen. 185 (1999) 293.
[34] C.-H. Lin, C.-Y. Hsu, J. Chem. Soc., Chem. Commun. (1992) 1479.
[35] F. Arena, R. Dario, A. Parmaliana, Appl. Catal. A: Gen. 170 (1998) 127.